Available online at www.elixirpublishers.com (Elixir International Journal)

Electrical Engineering

Elixir Elec. Engg. 42 (2012) 6313-6319

ISSN: 2229-712X

PWM based resonant converter with improved input power factor for power supply units

Y.Sukhi[1] and Y.Jeyashree[2]

[1]Department of EEE, RMK Engineering College, Kavaraipettai, Chennai, TamilNadu

[2]C&I Department, SRM University, Kattangulathur, Chennai, Tamil Nadu.

ARTICLE INFO

Article history:

Received: 15 November 2011;

Received in revised form:

2 January 2012;

Accepted: 16 January 2012;

Keywords

Power factor correction (PFC),
Resonant converter,
Zero voltage switching (ZVS),
Pulse width modulation(PWM),
Total harmonic distortion.

ABSTRACT

This paper presents a microcontroller based series parallel resonant converter suitable for the single stage single phase power factor correction circuits. The performance of the proposed converter is improved from no-load up to full-load. The steady state characteristics of the proposed converter are developed and a design example is given in detail. The proposed converter allows zero voltage switching at any loading condition with a reasonable power factor and with a promising efficiency. Simulation and experimental results verify the analysis made and the design specifications.

Introduction

In search of low cost high power factor power supply units, several reduced component count topologies have been proposed [1]. A power supply unit when extracting power from ac-line source needs a diode rectifier bridge with bulk capacitor to provide a smooth dc- link voltage for the high frequency inverter stage. Such a inverter circuit inevitably draws a high peak input current, which is of very poor factor and serious harmonic distortion. Therefore, with the growing concern on the input power quality, a filter circuit for power factor correction and harmonic reduction becomes a requirement.

At high power levels, full bridge (FB) zero voltage switching (ZVS) phase shifted DC-DC converter has been an attractive choice, since it provides high power density with high efficiency and low electromagnetic interference[2]. Also, this converter incorporates the advantages of low conduction losses present in hard switched topology, as well small switching losses provided by soft switching losses. Most conventional power factor correcting systems introduced so far employ pulse width modulation techniques to achieve the features of the PFC converter mentioned above.

However, the anxious trend to have a more compact power supply encourages higher operating frequencies. In this context, the PWM converters fall short to work at such high frequencies as the parasitic elements establish an enormous stress on the circuit elements associated with a noticeable electromagnetic interference (EMI) noise.

Resonant converters are known to be superior to PWM converters at high frequencies as it can compensate the parasitic elements effects within the resonant tank elements. They enjoy single-stage construction, lossless switching along with a minimized EMI noise [3]. On the other hand, single stage ac–dc resonant converters suffer the dependency of the zero voltage switching (ZVS) capability on the loading conditions, which needs a large regulating frequency range under the conventional variable frequency (VF) control [4]. The resonant circuit has succeeded in optimizing the size of the converter elements and acquiring a better efficiency [5]. In [6], a first step was taken to recommend the use of either the parallel or series-parallel resonant converters for single stage single phase PFC. However, the series-parallel is recommended for its lower component stress.

In [7], there was a suggested control scheme that swallows the need of the input current sense by sensing the input voltage only to simplify the controller structure via reducing the measurement effort but unfortunately it requires adding a hard limiter to control the peak of the control voltage signal to prevent its susceptibility to noise.

From the point of view of control theory, this is considered a major drawback as the existence of hard limiters imposes some limitations on both the input voltage range as well as loading range.

In addition, the controller in [8] was adjusted to lower the total harmonic distortion (THD) at certain operating points using a fixed-gain scheme, this fixed-gain scheme is calculated by a trial and error process, which does not guarantee a robust controller design.

In order to avoid the aforementioned drawbacks, this paper suggests a modified microcontroller, which does not need the input current measurement and ability to achieve the standard design specifications.

The suggested microcontroller operates to force the input current to follow the input voltage to achieve unity power factor under all loading conditions. This control gathers the advantages of obtaining ZVS without dependency on the load and unity power factor under all loading conditions. Design guidelines are given along with an example of a 500-W single stage single phase ac–dc converter operating from a universal 100–230 V rms, 50-Hz supply with a 50V dc output.

Tele:
E-mail addresses: sukhirmk03@yahoo.com

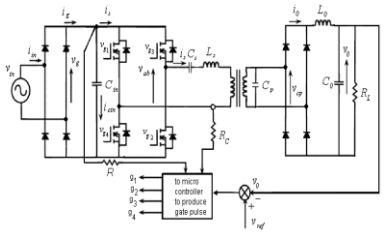

Fig. 1. Proposed converter

From the circuit diagram in Fig. 2, it is given that

$$i_g = i_s + i_{cin} = i_s + C_{in}\frac{dv_g}{dt} \quad (1)$$

Sensing the resonant current i_s and the rectified input voltage V_g , the input current can be calculated. This will enable the controller to track the input current reference according to any variation of the load or the input voltage. In other words, the controller will adjust itself automatically to generate the corresponding input reference current that corresponds to the condition of input voltage or load to control the power flow like in the current mode control without the need of sensing the input current.

Circuit Operation and Design

The proposed ac–dc converter employs a full bridge series parallel resonant converter with an inductive capacitive output filter as shown in Fig.1. It consists of an uncontrolled diode full-bridge rectifier followed by a small dc link capacitive filter C_{in} as a high frequency bypass, therefore, the input voltage to the resonant tank and the inverter is a rectified line voltage. It is important to mention that the resonant current i_s as a feedback signal, which is summed up with the derivative of V_g to generate i_g instead of measuring it. In fact, if a sinusoidal current is drawn from the ac input line, the power delivered by the converter to the output filter together with the load has a wave shape of a double frequency sinusoid with a peak value equal to twice the average.

Since, there are only two fundamental frequencies in the circuit, one is the line frequency (50 Hz), and the other is the switching frequency, which ranges from 100 to 150 kHz in our converter as will be explained in the following sections. It is assumed that the input source to be a dc source with an average value equal to the peak value of the ac source that will supply an average power double that of the ac source [9].

As a result, the converter design will be the same procedure of designing a dc–dc converter. The design specifications of the proposed ac–dc converter are as follows:

1) input voltage range (100–230 V rms, 50 Hz) Output voltage 50V

2) output power of the converter at full-load (500 W)

3) minimum switching frequency (100 kHz).

The operation of the converter must satisfy the following mathematical relation

$$V_0 = \frac{2\sqrt{2}V_{ab}\sin\gamma/2}{\pi\times\left[\left(\frac{\beta+1}{\beta}\right)\left(1-\alpha^2\right)+\frac{8}{\pi^2}\,jQ_S\left(\alpha-\frac{1}{(\beta+1)\alpha}\right)\right]} \quad (2)$$

where β is the ratio between the series and the parallel resonant capacitors at the primary side C_s, and C_p, respectively, Q_s is the resonant tank quality factor, α is normalized switching frequency.

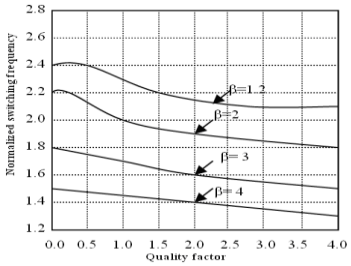

Fig. 2. Switching frequency ratio versus Quality factor Q_s.

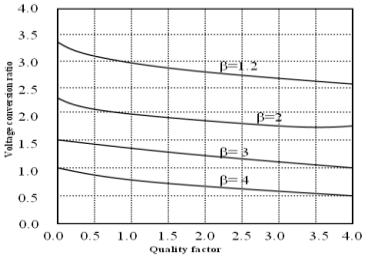

Fig. 3. Voltage gain of the converter versus Quality factor Q_s.

Fig. 2 shows the switching frequency ratio α obtained for various values of quality factor Q_s In order to avoid solutions that are associated with operation below the resonant frequency, the following constraint on the switching frequency ratio α must be considered:

$$\alpha > 1 \quad (3)$$

Input-Output Power Balance Constraint and Quality Factor

When a loss-less resonant circuit is in sinusoidal steady-state operation, the average power sent by the inverter to the resonant circuit, p_{in}, over one switching interval, is equal to the averaged power delivered by the resonant circuit to the output stage, p_o. Therefore, the quality factor Q_s can be expressed in terms of the output voltage and input power in the following way:

$$Q_s = \frac{\omega_0 L_s}{R_L} = \frac{\omega_0 L_s p_{in}}{v_0^2} \quad (4)$$

In this section, a procedure to obtain the currents, as well as the voltages in the resonant converter when the circuit Fig. 1 operates with unity power factor and constant output voltage is presented. This procedure will be used for the derivation of the design curves required for the selection of the power circuit components.

Operation with Unity Input Power Factor

When single phase converters, as the one shown in Fig. 1, are operated with unity input power factor, they draw a sinusoidal current from the ac mains that are in phase with the incoming ac voltage. Therefore, the input power is

$$p_{in} = P_{in,\max}\sin^2(\omega t) \quad (5)$$

where ω is the frequency of the ac mains expressed in radians per second. Noting that the switching frequency is much higher than the ac mains frequency, usually more than 1000, it is reasonable to assume that the resonant circuit is in steady-state operation at each point along the input line cycle. Therefore, the static characteristics derived in the previous section can be used to investigate the operation of the ac–dc converter of Fig.1.

As the power absorbed by the converter changes along the input line cycle, the quality factor Q_s also changes. The quality factor Q_s can be obtained by substituting (5) into (4), i.e.,

$$Q_s = \frac{\omega_0 L_s}{v_0^2} P_{in,\max}\sin^2(\omega t) = Q_{s\max}\sin^2(\omega t) \quad (6)$$

A procedure to find the maximum voltage conversion ratio of the ac–dc resonant converter has to be defined since both the input voltage v_g and the quality factor Q_s change along the input line cycle. In order to define this procedure, the first step is to identify the control angle at the resonant frequency. For the operation of the resonant circuit with lag power factor, the control angle must satisfy 90°<γ <180 [1]. On the other hand, it is desirable to switch the converter above the resonance frequency, since in this range the sign of the gain of the converter does not change. With the maximum value of the angle γ defined as 180, the maximum voltage conversion ratio as a function of the can be found by solving (2) for given values of Q_s. The resulting curves, which summarize the maximum voltage conversion ratio of the ac–dc converter, are given in Fig.3.

Design Procedure For The Converter Parameters

The following procedure is suggested for the selection of the resonant circuit parameters.

i) From Fig. 3, select the values of Q_s and β and also β should be chosen corresponding to a low voltage ratio to avoid large transformer ratio. For example, Q_s=2.94 and β=4 result in a maximum voltage conversion ratio M=0.6. The minimum switching frequency ratio that corresponds to this value of Q_s and β can be found from Fig. 2, that is α=1.36. From Fig. 2 it can be deduced that the maximum predicted switching frequency will be around 1.5 times the resonant frequency taken at nominal input voltage. This feature will be assured with the simulation results of the prototype.

ii) Select the minimum switching frequency and compute the series resonant inductor and the resonant capacitors. For example, if the minimum switching frequency is 100 kHz the resonant frequency can be found as follows:

$$\omega_0 = \frac{\min(\omega_s)}{\alpha} = 73.52\times10^3 rad/s \qquad (7)$$

The series resonant inductor is found by solving (12) for L_s, that is

$$L_s = \frac{Q_s \dfrac{M_m^2 v_{gm}^2}{P_{in}}}{\omega_0} = 38\mu H \qquad (8)$$

where P_{in} is made equal to twice of 500 W and the peak value of the lowest input voltage, which is (141.42 V) in this case. The value of the series resonant capacitor and the parallel resonant capacitor reflected to the primary side of the transformer are

$$C_s = \frac{1}{\omega_0^2 L_s} = 24.2nF \qquad (9)$$

$$C_p = \frac{C_s}{\beta} = \frac{24.2\times10^{-9}}{4} = 6.05nF \qquad (10)$$

iii) Select the turns ratio of the isolation transformer to step down the output voltage (v_0) to the value required at the output of the converter. The dc output voltage for operation without isolation transformer is given by

$$v_0 = M_m v_{gm} = 115.96V \qquad (11)$$

Therefore, for an output voltage equal to 50 V the turns ratio of the transformer is

$$\frac{n_1}{n_2} = \frac{115.96}{50} = 2.3 \qquad (12)$$

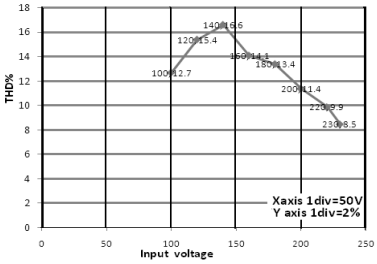

Scale: x-axis 1div=50Vy-axis 1div=2%
Fig. 4. %THD versus input voltage at full-load.

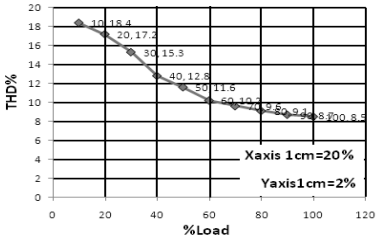

Scale:x-axis 1div=20% y-axis 1div=2%
Fig. 5. %THD versus % load at Vin=230V.

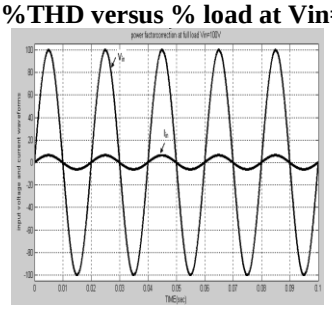

Scale: x-axis 1div=0.01sec
y-axis 1div=20V, y-axis 1div=20A
Fig.6 Input voltage and current waveforms at full load with 100V_{rms} input voltage

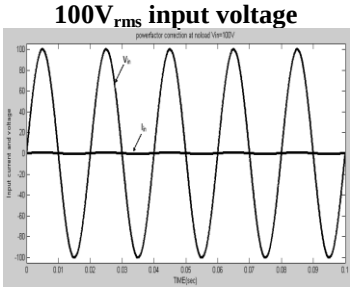

Scale : x-axis 1div=0.01sec
y-axis 1div=20V, y-axis 1div= 20A
Fig.7 Input voltage and current waveforms at no load with 100V_{rms} input voltage

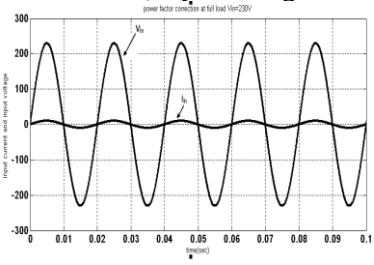

Scale: x-axis1div=0.01sec
y-axis 1div=100V , y-axis 1div=100A
Fig.8 Input voltage and current waveforms at full load with 230V_{rms} input voltage

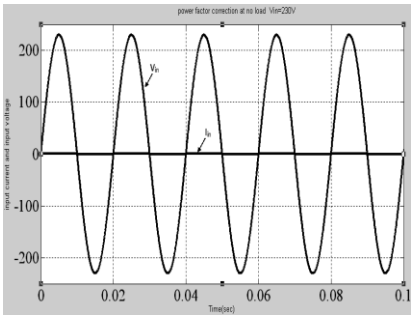

Scale: x-axis1div=0.02sec, y-axis 1div=100V , y-axis 1div=100A

Fig.9 Input voltage and current waveforms at no load with 230V_{rms} input voltage

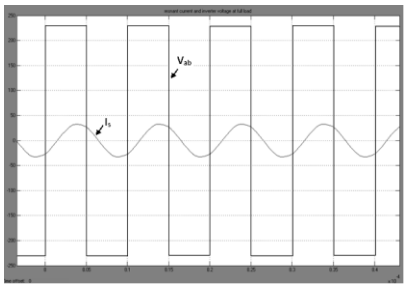

Scale: x-axis1div=5µsec y-axis1div=50V , y-axis1div=50A

Fig. 10 ZVS at 230V under full load

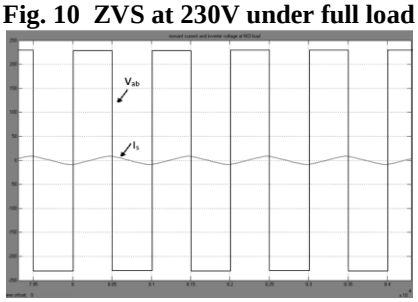

Scale: x-axis1div=5µsec y-axis1div=50V, y-axis1div=50A

Fig.11 ZVS at 230V under no load

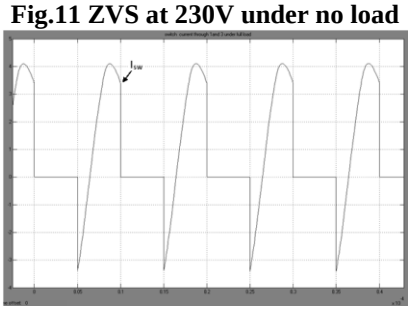

Scale: x-axis 1div=5µsec y-axis 1div=1A

Fig.12 switch current through 1 and 3 at 230V under full load

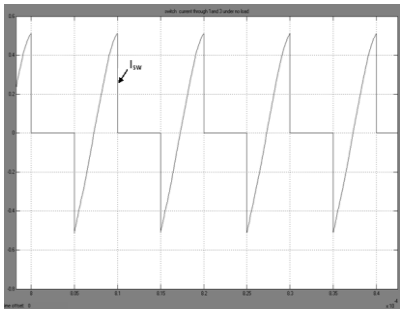

Scale: x-axis 1div=5µsec y-axis 1div=0.2A

Fig.13 switch current through 1 and 3 at 230V under no load

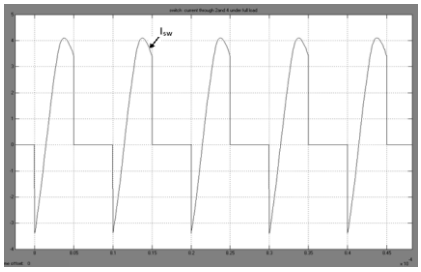

Scale: x-axis 1div=5µsec y-axis 1div=1A

Fig.14 switch current through 2 and 4 at 230V under full load

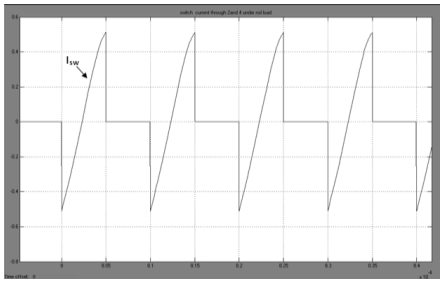

Scale: x-axis 1div=5µsec y-axis 1div=0.2A

Fig.15 switch current through 2 and 4 at 230V under no load

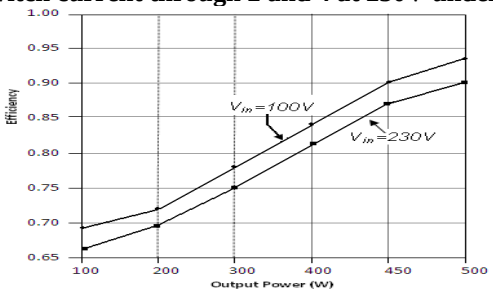

Scale: x-axis1div=100W y-axis1div=0.05

Fig.16 Overall converter efficiency versus load condition: different input voltages

Simulation Results

Simulation of the proposed single stage PFC converter is performed under MATLAB software in order to validate the design procedure illustrated above. Table I shows the converter parameters used in the layout.

Input Power Factor

Recorded waveforms of the input voltage and current in Fig. 6 and Fig.7 indicate that the proposed converter has a very good input power factor ranging from 0.985 at no-load to 0.965 at full-load at nominal input voltage of 100 V_{rms}. Fig. 8 and Fig.9 verifies that the input current waveform follows the input voltage waveform under all of the possible loading conditions at an input voltage of 230 V rms.

The THD of the input current is also presented for different input voltages at full-load and presented in Table II. Fig.4 explains that the %THD variations for various values of input voltages. Also, the input current THD recordings were taken at different loading conditions at the rated input voltage of 230 V_{rms} and presented in Table III. Fig. 5 shows that the required design specifications are met at any loading conditions. In both Tables II and III, the %THD is under any condition is found to be less than 18%.

Zero Voltage Switching (ZVS)

Fig. 10 and Fig.11 show the waveforms of the resonant current, switch current and inverter output voltage at different operating conditions. The resonant current always lags the inverter output voltage and crosses zero inside of the non-zero voltage pulse at output of the inverter, resulting in the required

current to reset the snubber capacitors and provide ZVS. Fig. 12 to Fig.15 shows the waveforms of the switching currents at different operating conditions.

Performance Characteristics

Fig. 16 illustrates the variation of the working efficiency with output load power for different input voltages. Its efficiency is in direct proportion with the load. However, this is due to the circulating current conduction loss in the resonant tank

Switching Frequency Range

It is known that the proposed method is advantageous over the conventional control with a reduced switching frequency range. The proposed method provides a significant reduction in the switching frequency range than that of the conventional method from no-load up to full-load at both input voltage extremes: 100 and 230 V.

With the proposed method, the operating frequency range can be reduced to about 50% when compared with the conventional method as shown in Fig. 17 and Fig.18. The reduction in the switching frequency leads to a decrease in the magnetic losses of the resonant inductor and the transformer, also a decease in the frequency dependent losses of the controller, and a more compact size converter components.

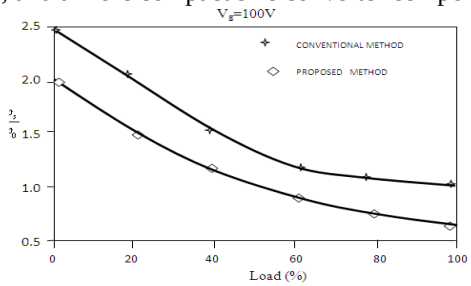

Scale: x-axis 1div=20% y-axis 1div=0.5
Fig.17 switching frequency variation at different loading conditions for V_g = 100 V.

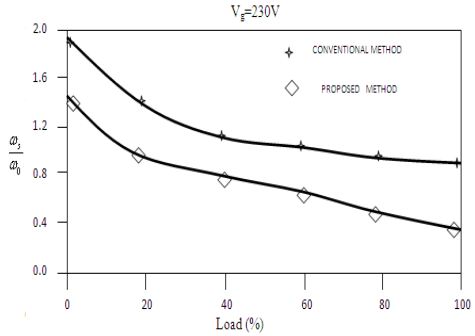

Scale: x-axis 1div=20% y-axis 1div=0.4
Fig.18 switching frequency variation at different loading conditions for V_g = 230 V.

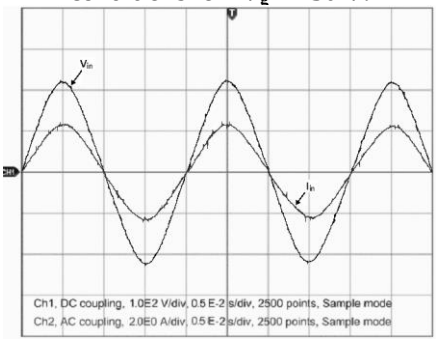

Scale: x-axis 1div=0.05sec,
y-axis 1div=100V, y-axis 1div=2A
Fig.19 Input current and voltage waveforms

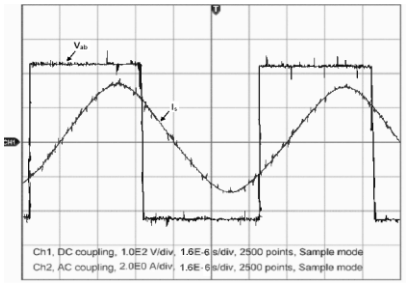

Scale: x-axis 1div=1.6µsec
y-axis 1div=100V, y-axis 1div=2A
Fig.20 ZVS at full-load for V_g=230V

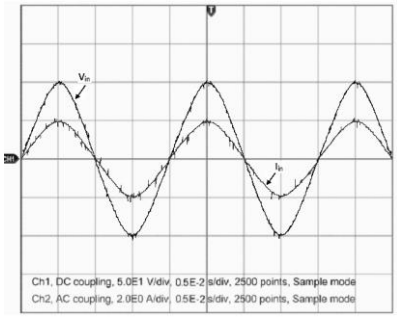

Scale: x-axis 1div= 0.05sec
y-axis 1div=50V, y-axis 1div=2A
Fig.21 Input current and voltage waveforms

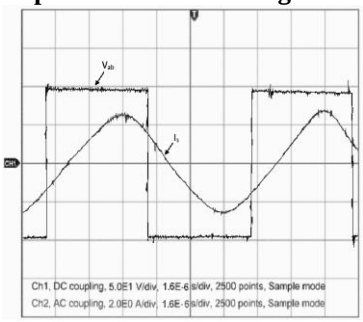

Scale: x-axis 1div=1.6µsec
y-axis 1div=50V, y-axis 1div=2A
Fig.22 ZVS at full-load for V_g=100V

Experimental Results

This section aims to validate the concepts developed in the previous sections. This section is intended to highlight the compliance of the proposed converter with the desired design specifications: ZVS, high input power factor at different loading conditions and input voltage values and the narrow range of the switching frequency of the converter.

Zero Voltage Switching (ZVS)

Typical inverter output voltage and current for operation are shown in Fig. 20 and Fig.22. It was verified experimentally that the current always crosses zero inside of the non-zero voltage pulse at output of the inverter, resulting in the required current to reset the snubber capacitors and provide ZVS at full-load.

Input Power Factor and Efficiency

Fig. 20 and Fig. 22 show the converter capability to achieve ZVS at V_g= 230V and also at V_g=100V respectively. The resonant current possesses the same polarity as it lags the inverter output voltage, which enables the ZVS as explained before.

Fig. 19 and Fig. 21 illustrate the corresponding input voltage and current waveforms at V_g= 230V and also at V_g=100V respectively. Fig. 16 illustrates the variation of the working efficiency with output load power for different input

voltages. Its efficiency is in direct proportion with the load. However, this is due to the circulating current conduction loss in the resonant tank.

Conclusion

This paper presents a new front-end ac–dc power supply based on the series parallel resonant converter using microcontroller. The microcontroller does not require the input current measurement, which allows a smaller size filter because of the absence of the input inductor. In addition, it is capable of adaptively adjusting the reference current according to the loading condition or the input voltage variation. A detailed design procedure has been given to select the values of the resonant components for a design case. Simulation and experimental results show that the proposed converter enjoys a high input power factor, low input current THD together with a ZVS capability and high efficiency.

References

1. Junming Zhang, Xiaogao Xie, Xinke Wu, Guoliang Wu, and Zhaoming Qian, A Novel Zero-Current-Transition Full Bridge DC/DC Converter IEEE Transactions on Power Electronics, Vol. 21, No. 2, March 2006 pp: 354-361.

2. Staffan Norrga Experimental Study of a Soft-Switched Isolated Bidirectional AC–DC Converter Without Auxiliary Circuit IEEE Transactions on Power Electronics, Vol. 21, No. 6, November 2006 pp: 1580-1588.

3. Yungtaek Jang, Milan M. Jovanovic , and David L. Dillman Soft-Switched PFC Boost Rectifier With Integrated ZVS Two-Switch Forward Converter IEEE Transactions on Power Electronics, Vol. 21, No. 6, November 2006 pp:1600-1607.

4. Mohamed Z. Youssef, , and Praveen K. Jain, A Novel Single Stage AC–DC Self-Oscillating Series-Parallel Resonant Converter IEEE Transactions On Power Electronics, Vol. 21, No. 6, November 2006 pp: 1735-1745.

5. Xinke Wu, Junming Zhang, Xiaogao Xie, and Zhaoming Qian Analysis and Optimal Design Considerations for an Improved Full Bridge ZVS DC–DC Converter With High Efficiency IEEE Transactions On Power Electronics, Vol. 21, No. 5, September 2006 pp: 1225-1235.

6. Junhong Zhang, Jih-Sheng Lai, Rae-Young Kim, and Wensong Yu High-Power Density Design of a Soft-Switching High-Power Bidirectional dc–dc Converter IEEE Transactions on Power Electronics, Vol. 22, No. 4, July 2007 pp:1145-1154.

7. Xiaogao Xie, Junming Zhang, Chen Zhao, Zhuo Zhao, and Zhaoming Qian, Analysis and Optimization of LLC Resonant Converter With a Novel Over- Current Protection Circuit IEEE Transactions on Power Electronics, Vol. 22, No. 2, March 2007 pp:435-444.

8. Andrew J. Mason, Darryl J. Tschirhart, and Praveen K. Jain, New ZVS Phase Shift Modulated Full-Bridge Converter Topologies With Adaptive Energy Storage for SOFC Application IEEE Transactions On Power Electronics, Vol. 23, No. 1, January 2008 pp:332-343.

9. Yan Lu, K. W. Eric Cheng, and S. L. Ho Quasi Current Mode Control for the Phase-Shifted Series Resonant Converter IEEE Transactions on Power Electronics, Vol. 23, No. 1, January 2008 pp: 353-359.

TABLE I
Converter parameters for the proposed power supply

Component	value
Switches	IRF640
L_s	38µH
C_s	24.2nF
C_p	6.05 nF
$n_1:n_2$	2.3:1
C_{in}	60µF
C_0	100µF
L_0	0.1mH

TABLE II THD levels of the input current for different input voltage at full-load

RMS Input Voltage	%THD
100	12.7
120	15.4
140	16.6
160	14.1
180	13.4
200	11.4
220	9.9
230	8.5

TABLE III THD levels for different loading conditions at rated input voltage

%Loading	%THD
10	18.5
20	17.5
30	15.3
40	12.8
50	11.6
60	10.2
70	9.6
80	9.1
90	8.7
100	8.5